Current Research in Food Science 5 (2022) 1127–1139

Contents lists available at ScienceDirect

Current Research in Food Science

journal homepage: www.sciencedirect.com/journal/current-research-in-food-science

# Regulatory mechanisms of the green alga *Ulva lactuca* oligosaccharide via the metabolomics and gut microbiome in diabetic mice

Yihan Chen [b,1], Weihao Wu [b,1], Xiaoyu Ni [b], Mohamed A. Farag [e], Esra Capanoglu [f], Chao Zhao [a,b,c,d,*]

[a] College of Marine Sciences, Fujian Agriculture and Forestry University, Fuzhou, 350002, China
[b] College of Food Science, Fujian Agriculture and Forestry University, Fuzhou, 350002, China
[c] Engineering Research Centre of Fujian-Taiwan Special Marine Food Processing and Nutrition, Ministry of Education, Fuzhou, 350002, China
[d] Key Laboratory of Marine Biotechnology of Fujian Province, Institute of Oceanology, Fujian Agriculture and Forestry University, Fuzhou, 350002, China
[e] Pharmacognosy Department, College of Pharmacy, Cairo University, Cairo, Egypt
[f] Department of Food Engineering, Faculty of Chemical and Metallurgical Engineering, Istanbul Technical University, Maslak, 34469, Istanbul, Turkey

ARTICLE INFO

Handling editor: Alejandro G. Marangoni

*Keywords:*
Type 2 diabetes
*Ulva lactuca* oligosaccharide
Senescence
Differential metabolite
Gut microbiota

ABSTRACT

Type 2 diabetes (T2D) has emerged as one of the most acute public health diseases of the present time, which increases with the population ageing. This study aimed to evaluate the hypoglycaemic activity of *Ulva lactuca* oligosaccharide (ULO) under ageing-related diabetes conditions in an animal model. The results demonstrated that ULO can promote hypoglycaemia and delay senescence as mediated *via* GLP-1/GLP-1R pathway to mobilize the intercommunication between the brain and gut. In addition, twenty-six different metabolites and eight different bacteria were screened in the brain and the gut, respectively. A network relationship displayed that all-trans-retinoic acid has positive relationships with *Bifidobacterium* and *Streptococcus*, suggesting that plays a potential key role in maintaining the hypoglycaemic and anti-ageing activities of ULO. Based on these findings, ULO might be an efficient therapy for restoring blood glucose metabolism and delaying brain senescence in elderly T2D patients.

## 1. Introduction

As older populations continue to increase worldwide, there is a growing demand for evidence to determine the potential molecular mechanisms that drive ageing-related diseases, such as type 2 diabetes (T2D), cancer, and cardiovascular disease. There are more than 463 million definite cases of T2D, and the estimated number of diabetic cases is expected to reach 700.2 million, in which T2D cases over the 65 years old account for 39.44% by 2045. (Sinclair et al., 2020). As a type of chronic degenerative disease, T2D, characterized by hyperglycaemia, insulin resistance, and related comorbidities, is driven by dysfunction of insulin secretion and impaired β-cells function (Zhao et al., 2020a,b,c). Currently, all therapeutic measures for T2D share the common objective of decreasing blood glucose level, *i.e.*, by stimulating insulin secretion, improving glucose intake in the peripheral organs, and enhancing the consumption of liver glucose (Ghislain and Poitout, 2021; Zhao et al., 2020a,b,c). Intriguingly, enteroendocrine hormone glucagon-like peptide 1/glucagon-like peptide 1 receptor (GLP-1/GLP-1R) agonists have been proposed recently as a novel therapeutic measure for stimulating insulin secretion. Prior evidence has demonstrated that GLP-1/GLP-1R agonists are highly efficacious in controlling blood glucose level, food intake, and obesity (Nauck et al., 2009). While the brain plays a key role through the autonomic nervous system and the hypothalamic-pituitary-adrenal axis to influence many gastrointestinal processes, including motility and transport, fluid and mucus secretion, immune activation, intestinal permeability, and the relative abundance of intestinal microbes (Osadchiy et al., 2019). In addition, the change in intestinal microenvironment can lead to the variation of the gut microbial community, including the bacteria species abundance and function. Meanwhile, the gut flora can feed back to the brain through hundreds of metabolites to transmit neural signals to maintain homeostasis of systemic function (Gupta et al., 2020). Prior evidence has uncovered that the risk of Alzheimer's disease and vascular dementia significantly enhanced in T2D patients, accompanying the weakening of

* Corresponding author. No.15 Shangxiadian Road, Fuzhou, 350002, China.
*E-mail addresses:* mohamed.farag@pharma.cu.edu.eg (M.A. Farag), zhchao@live.cn (C. Zhao).
[1] Yihan Chen and Weihao Wu contributed equally to this study.

https://doi.org/10.1016/j.crfs.2022.07.003
Received 16 April 2022; Received in revised form 15 June 2022; Accepted 1 July 2022
Available online 14 July 2022

the function of the central nervous system (Bosco et al., 2012). Especially in ageing individuals, the brain seems to be more susceptible to cell-intrinsic and local signals that suggest sped up or slowed ageing process (Kaplan et al., 2020).

Metabolites represent both the genome's downstream outputs and the environment's upstream inputs, enabling scientists to explore the nexus of gene and environmental interactions. As an emerging systems biology approach, metabolomics is now widely used in clinical and biomedical research to understand and construct blueprints of pathophysiological processes and search for diagnostic and prognostic biomarkers for various organisms (Huang et al., 2021). Metabolic profiling and metabolic phenotyping can predict ongoing pathological processes, identify disease biomarkers as endogenous and exogenous metabolites, and provide unique insights into disease etiology (Serag et al., 2021). Prospective studies have shown that patients with T2D exhibit higher levels of carbohydrate (glucose and fructose), lipid (phospholipids, sphingolipids, and triglycerides) and amino acid (branched-chain amino acids, aromatic amino acids, glycine, and glutamine) metabolites than the healthy population (Guasch-Ferré et al., 2016). In contrast, serine, glutamine, and lysophosphatidylcholine C18:2 reduced the risk of T2D progression. The increasing advances in metabolomics expect to aid uncover novel markers or drug targets in diabetes and ageing treatment.

The accumulated evidence shows that natural bioactive resources have great anti-diabetes and anti-aging potential (Agunloye and Oboh, 2022; Tundis, 2021). The green algae have great potential in natural agent resource mining, attracting many scientists owing to their special bioactivities. *Ulva lactuca*, a kind of green algal referred to as class Chlorophyceae, is rich in polysaccharides, proteins, vitamins, and several other phytonutrients (Liu et al., 2019). Especially polysaccharides have been discovered many potential bioactivities for anti-ageing, anti-tumor, and anti-diabetic efficacy (Liu et al., 2019; Teferra, 2021). Emerging studies have suggested that *U. lactuca* polysaccharide (ULP) can enhance the immunomodulatory capacity against tumor growth in H22 hepatoma-bearing mice (Zhao et al., 2020a,b,c). However, polysaccharides have been limited for their large molecular weight and inability to take part directly in complex cellular metabolic processes. Our previous study has revealed that ULO possesses significant hypoglycaemic and anti-ageing efficacy for *Caenorhabditis elegans* with insulin resistance induced by high glucose level (Wu et al., 2020). However, the complex mechanisms of ULO for both hypoglycaemia and anti-ageing activities have not been well studied in mice. The gut-brain-liver axis has been increasingly recognized as a new theory to treat obesity and diabetes (Beraza and Trautwein, 2008), and whether polysaccharides can mediate for their biological effects through such axis has yet to be examined. This study aimed to determine the underlying correlation between brain metabolites and gut microbiota at multi-cellular levels by monitoring metabolites changes *via* multi-omics analysis, providing a novel perspective for exploring the molecular mechanism of ageing-related diabetes.

## 2. Material and methods

### 2.1. Animals

Fifty male ICR mice (6 weeks old, 35 ± 5 g) were purchased from Wu's Laboratory Animal Co., Ltd. (Fuzhou, China) and raised according to the ethics review process and the regulations of the Welfare Committee of Fujian Agriculture and Forestry University (Ethical approval number PZCASFAFU21001). Firstly, the temperature and humidity were set at 25 °C and 55%, respectively. All animals were adapted for one week and provided a normal diet and water. After that, animals were randomly divided into 5 groups: the normal feed group (Normal), the ageing-related diabetic group (Model), the metformin group (Met, 100 mg/kg/d), the low dose of ULO (ULOL, 150 mg/kg/d), and the high dose of ULO (ULOH, 300 mg/kg/d). Specifically, except for the normal group, animals continuously underwent 30 days of intraperitoneal injection with D-galactose (D-Gal, 45 mg/kg/d) and were fed a high-fat diet. Next, mice were simultaneously injected with the low dose streptozotocin (STZ, 45 mg/kg) and D-Gal for 10 days. The injection of STZ was limited to once every 3 days, and fast blood glucose (FBG) was tested before the next injection until the fasting blood glucose level of all animal experiments exceeded 11.0 mmol/L. Oral intervention was carried out at the same time every day for four weeks until the end of the trial. Next, animals were fasted for 12 h, anaesthetized with 1% sodium pentobarbital solution, and then removed the neck quickly after taking blood from the eyeball.

### 2.2. Sample collection and biochemical parameter analysis

The FBG level was determined every two weeks, and the body weight change was recorded to analyze the effects caused by ULOL and ULOH. Using the method from Lin et al. (2021a), oral glucose tolerance was measured from 0 to 120 min. All samples, including the brain, liver, and jejunum, were collected and stored at −80 °C for the subsequent analysis. The fresh liver tissues (100 mg) were broken and dissolved in 0.9% saline and then centrifuged at 8500 rpm for 10 min at 4 °C. The liquid supernatant was subsequently collected, and the levels of catalase (CAT), total superoxide dismutase (T-SOD), malondialdehyde (MDA), and glutathione peroxidase (GSH-PX) were measured using assay kits (Jiancheng Biotechnology, Nanjing, China). Liver insulin level was determined using ELISA assay kit following manufacturer protocol (Jiangsu MeiBiao Biological Technology Co., Ltd.)

### 2.3. Histopathological examination

The liver, jejunum, and brain tissues stained with hematoxylin and eosin (H&E) stain for the histopathological examination. Specifically, these tissues were put into the 4% paraformaldehyde and embedded in the paraffin, cut into 2 mm sections and stained, which was observed by the high-resolution microscope.

### 2.4. Real-time quantitative PCR assay

An ultrapure RNA kit (Gene-Better, Beijing, China) was used to extract the total RNA from the gut and brain. Using the method provided by the PrimeScript™ RT reagent kit with gDNA Eraser (Takara, USA) to synthesize the cDNA, the concentration of cDNA was detected by a NanoDrop One Microvolume UV–Vis Spectrophotometer (Thermo Fisher, USA). NovoStart® SYBR Green Color qPCR SuperMix (Novoprotein, Shanghai, China) was used for qPCR and then analyzed by the ABI7300 (Applied Biosystem, USA). Information of PCR primers is listed in Table S1.

### 2.5. Western blot assay

The proteins of gut and brain tissues were extracted by cell lysis buffer for Western blot and IP (Beyotime, Nanjing, China) and a suitable amount of phenylmethanesulfonyl fluoride (PMSF) was added to prevent against protein degradation (Beyotime, Nanjing, China). Subsequently, the protein concentration was measured using a BCA Protein Assay Kit (Beyotime, Nanjing, China), and protein concentration was diluted to 30 μg/10 μL in cell lysis buffer for Western blot and IP with 5 × SDS-PAGE sample loading buffer (Beyotime, Nanjing, China). Following the protocol described in Wan et al. (2020), protein expression levels from brain and gut tissues were detected targeting cyclin-dependent kinase inhibitor 2A ($p16^{Ink4a}$), forkhead box O1 (FoxO1), glucagon-like peptide 1 receptor (GLP-1R), matrix metallopeptidase 2 (MMP2), glucagon-like peptide 1 (GLP-1), glucose transporter type 4 (GLUT4), insulin receptor (INSR), and c-Jun N-terminal kinases (JNK) (Beyotime, Nanjing, China).

### 2.6. Sample preparation for non-targeted UPLC-MS metabolites profiling

Five milligrams of fresh mouse brain tissue were mixed with 500 μL methanol-water (Sigma-Aldrich Trading Co., Ltd, dilution of 80:20), and 10 μL of 100 μg/mL CA-d4 (CDN, Inc., CAN) internal standard was added. After that, the sample was swirled for 1 min and centrifuged at 13,000 rpm for 5 min at 4 °C. Then, 400 μL of supernatant was collected into a new centrifuge tube and the procedure described above was repeated. The supernatant was then blow-dried with nitrogen and then poured into the 100 μL ultrapure water, followed by centrifugation at 13,000 rpm for 5 min at 4 °C. The supernatant was then collected for subsequent analysis.

### 2.7. Metabolites profiling

An Ultimate 3000 apparatus coupled to Q-Exactive MS was used for the metabolomics analysis. Chromatographic separation was performed using an HSS T3 (100 × 2.1 mm, 1.8 μm, Waters). The positive ion mode flow phase was an aqueous solution containing 0.1% formic acid (A solution) and 100% methanol containing 0.1% formic acid (B solution). The anion mode flow phase was an aqueous solution (A solution) containing 10 mM of (A solution) and 95% methanol containing 10 mM of ammonia formate (B solution). The injection volume was 2 μL, the flow rate was 0.3 mL/min, and the column temperature was set at 35 °C. The detailed LC parameters were as follows: 10% B for 1 min; 98% B from 1 to 13 min; 98% B from 13 to 18 min; 10% B from 18 to 18.5 min and 10% B from 18.5 to 20 min. In addition, the positive and negative ions were scanned separately in MS mode with the following parameters: capillary temperature, 300 °C; detection mode, full mass/dd-MS2; resolution, 7000 for MS1 and 17,500 for dd-MS2; source voltage, 3.8 kV for positive and 3.2 kV for negative; sheath gas flow rate, 40 Arb; atomizer temperature, 350 °C.

### 2.8. Gut microbiota DNA extraction and sequencing

The QIAamp DNA Stool Mini Kit was used to extract fecal samples of DNA from mice and DNA sequence analysis was performed using Life Ion S5TM. A similarity of 97% was set as operational taxonomic units (OTUs), and species annotation was conducted. After that, Rstudio (Rstudio, Boston, USA) and Simca 14.1 (Umetrics, Sweden) were used to calculate and visualize the results.

### 2.9. Statistical analysis

All results are reported as the mean ± SD (n = 6). Statistical data were considered to be significantly different when the *P*-value was less than 0.05 or 0.01. Spearman's correlation coefficient was used to calculate the correlation between the gut microbiota and metabolites. In addition, the metabolite data were normalized using Pareto scaling and the main pathway analyzed was mapped upon KEGG database.

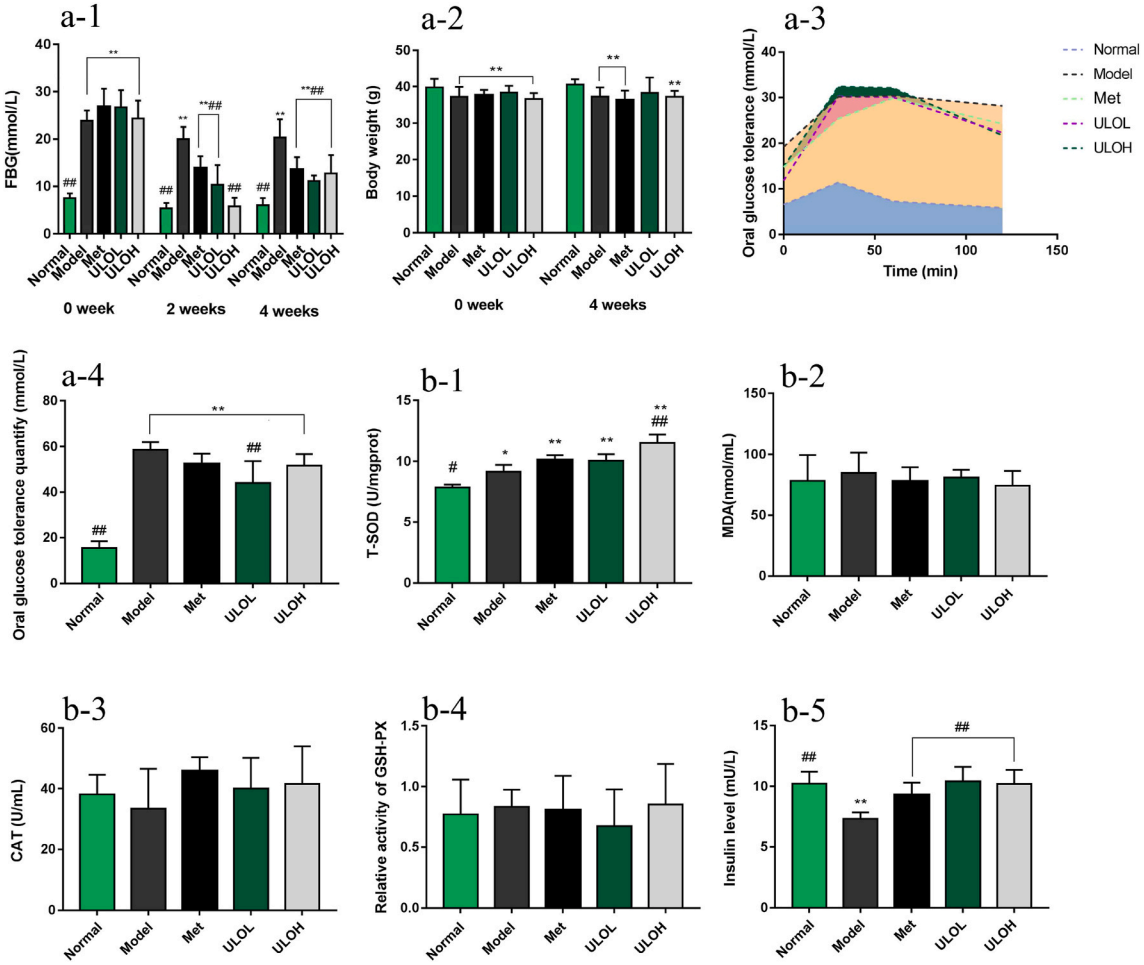


**Fig. 1.** The effects of ULO on FBG (a-1), body weight (a-2), oral glucose tolerance (a-3), and oral glucose tolerance qualify (a-4). The effects of ULO on liver T-SOD (b-1), MDA (b-2), CAT (b-3), GSH-PX (b-4), and insulin level (b-5). Compared with the normal group, $^{*}P < 0.05$, $^{**}P < 0.01$. Compared with the model group, $^{\#}P < 0.05$, $^{\#\#}P < 0.01$.

## 3. Results

### 3.1. Effects of ULO on the blood glucose related index and liver biochemical parameters

To assess the hypoglycaemic activity of ULO in ageing-related diabetic mice, FBG levels of animals were measured within 0–4 weeks of ULO intervention (Fig. 1a–). All intervention groups, including the model, Met, ULOL, and ULOH groups, showed a statistically significant difference from the Normal group. The levels of FBG exhibited a promising reduction after 2 weeks of intervention by agents ($P < 0.01$), in which the levels of ULOL and ULOH reflected excellent hypoglycemic activity compared with Met group. With the expanded intervention time, the FBG levels remained in a stabilized condition after ULOL and Met interventions for 4 weeks (Fig. 1a–). The body weight of the intervention groups was significantly reduced from 0 to 4 weeks compared with that of the normal group ($P < 0.01$). While the ULOL group was not significantly different at 4 weeks compared to that of the normal group (Figs. 1a–2). Meanwhile, the index of oral glucose tolerance was measured for assess the impairment condition of glucose metabolism at 4 weeks (Figs. 1a–3). Specifically, all mice were tested for blood glucose levels from 0 to 120 min after oral supplementing glucose (2 g/kg). Notably, the ability to control blood glucose in the ULOL group was better than that in the Met and ULOH groups (Figs. 1a–4). These results suggested that oral intervention with ULOL (150 mg/kg/d) had significantly improvement effect on controlling FBG level in ageing-related diabetic mice.

Reactive oxygen species (ROS) are side products produced by natural oxygen metabolites, over accumulated ROS levels can damage the normal cell structure and function, advancing the process of cell senescence and apoptosis. Inhibition of ROS over accumulation has been demonstrated to be an effective anti-ageing strategy (Hwang et al., 2014). Generally, cells can produce various non-enzyme and enzyme substances to inhibit the oxidation reaction to relieve the ROS accumulation (Scherz-Shouval and Elazar, 2011), such as T-SOD, MDA, CAT, and GSH-PX. Based on the above results, the effects of ULO on antioxidant activity in the liver were determined. Compared with the normal group, all intervention groups including the Met, ULOL, and ULOH groups, showed a distinct enhancement in the level of T-SOD (Fig. 1b–). In contrast, levels of MDA, CAT, and GSH-PX (Figs. 1b-2-4) were not significantly different between the normal and model groups. In addition, the insulin level in the liver was much higher than that in the model group and showed an obvious difference during the Met and ULO intervention ($P < 0.01$; Figs. 1b–5).

### 3.2. Histopathological analysis of liver, brain, and intestine

Compared with the model group of H&E-stained of the histopathological sections (Fig. 2a–), the ULOH group (Figs. 2a–5) displayed an integral profile with minor cell damage and with clean edges, and these cells arranged in a regulated manner. Notably, the histopathological section of the ULOL group (Figs. 2a–4) exhibited clean edges among the cells. However, it exhibited distinct and incomplete morphology in the liver with less inflammatory infiltration, similar to the Met group. The histopathological section of the jejunum showed an integral villus boundary in the ULOL and Met groups (Figs. 2b–3 & 2b-4); however, these jejuna retained slight inflammatory cell infiltration. Compared with the normal group, the structure of epithelial cells in the model group exhibited serious destruction, such as villus breakage, and the intestine wall disappeared. Notably, blood stasis was obvious in the model group, and the number of colloidal cells was significantly reduced (Fig. 2c–). Additionally, these colloidal cells were arranged in a disorderly manner. Intriguingly, these deficits were restored by supplementing either Met or ULO (Figs. 2c–4 & 2c-5), especially in the ULOL group, which exhibited a significantly enhanced number of colloidal cells that were uniformly distributed. Collectively, these results show that ULO intervention can restore the destructive conditions in the jejunum and brain caused by ageing-related diabetes.

### 3.3. The effects of ULO on glucose metabolism and ageing-related mRNA and protein expression in the brain and gut

To further uncover the potential anti-ageing and hypoglycaemic effects of ULO, the RT-qPCR and western blotting were used in brain and gut tissues to detect respective mRNA and protein expression levels. Notably, both mRNA (Fig. 3a) and protein levels (Fig. 3c and d) of $p16^{Ink4a}$ and MMP2 expression levels in the model group were significantly enhanced following D-Gal and STZ intervention. Intriguingly, such increase was significantly reversed after supplementing ULO ($P < 0.01$). In contrast, Met decreased the expression level of $p16^{Ink4a}$, whereas MMP2 was not restored to normal as in case of ULO. Regarding the regulation of the feeding behavior switch (Varela and Horvath, 2012), FoxO1 and GLP-1R were significantly improved after supplementation with ULO, and these changes also occurred in the Met group (Fig. 3a, c and d). Compared with the integral expression level, however, the ULO groups showed the best effects on controlling these factors.

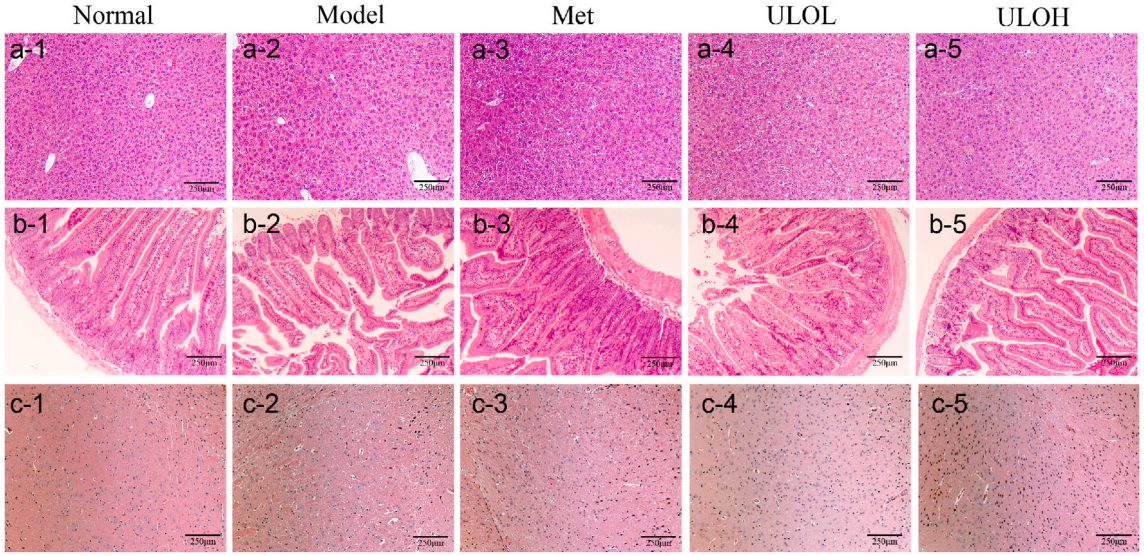


**Fig. 2.** Histopathological analysis of ULO on tissues under the H&E staining with 100 × magnification. The effects of ULO for liver (a), jejunum (b), and brain (c).

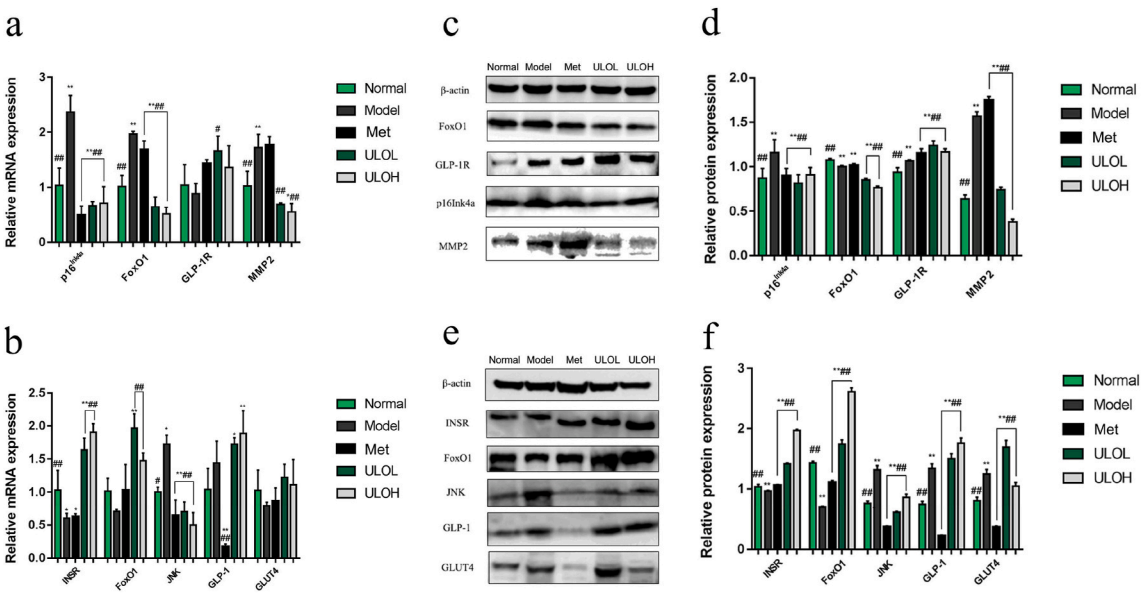


**Fig. 3.** The regulatory mechanism of ULO for mRNA and proteins in brain and gut. The relative mRNA (a) and protein expression levels in the brain (c–d). The relative mRNA (b) and protein expression levels in the gut (e–f). Compared with the normal group, $^{*}P < 0.05$, $^{**}P < 0.01$. Compared with the model group, $^{\#}P < 0.05$, $^{\#\#}P < 0.01$.

They play a key role in gut epithelial cells during the process of controlling blood glucose, especially insulin secretion and energy utilization. In the model group, insulin secretion-related mRNAs (Fig. 3b) and proteins (Fig. 3 and f), including INSR and JNK, changed in an adverse direction. Interestingly, supplementation with ULO seemed to protect against adverse conditions and significantly improved the expression of INSR and JNK ($P < 0.01$). Regarding energy utilization, ULO intervention increased the ability of cells to uptake energy, which was reflected in the expression of FoxO1 and GLUT4 ($P < 0.01$) (Fig. 3f). GLP-1, as the signal mediator between the brain and gut, is involved in the balance of blood glucose and promotes insulin secretion. The expression of GLP-1 significantly increased following ULO intervention, while the GLP-1 expression level was lowered after Met intervention, suggesting Met intervention may has hamper effect for GLP-1 secretion. In summary, these results showed a distinct change in molecular expression level, providing initial evidence for anti-ageing and hypoglycaemia activities of ULO.

### 3.4. The effects of ULOL on brain metabolites

Based on the above analysis, the brains from ULOL group were selectively chosen for the analysis of the metabolites being the most active as revealed from its effect on glucose metabolism and ageing-related mRNA and protein expression in the brain. The profiles of brain metabolites, including the normal, model, Met, and ULOL groups were detected by UPLC-MS in the ESI+ and ESI- modes. Partial least squares discriminant analysis (PLS-DA) and orthogonal partial least squares discriminant analysis (OPLS-DA) were further used to determine metabolites profile among groups using MetaboAnalyst 5.0 (https://www.metaboanalyst.ca/). According to the PLS-DA results, the profiles of brain metabolites were significantly changed after supplementing ULOL as detected in both ESI- (Fig. 4a) and ESI + modes (Fig. 4b). PLS-DA of all groups failed to show clear separation with significant overlap and poor variance coverage that is 32% and 50% in negative and positive modes, respectively. The only evident segregation in the PLS-DA with ESI- modes (Fig. 4a), was the segregation of the ULOL group along the positive coordinate direction even with slight overlap with the normal groups. The Met and model groups showed distributions more towards the negative coordinate direction. To further uncover the effects of the ULOL, OPLS-DA was adopted by model against normal, Met and ULOL each respectively one at a time in both negative (Fig. 4c, e and g) and positive modes (Fig. 4d, f and h). Notably, the ULOL group (Fig. 4g) showed a greater distance than the Met groups (Fig. 4e) in ESI- mode. The Met groups in ESI + mode (Fig. 4f) showed a significant distance from ESI-.

### 3.5. Identification of metabolite markers in the brain in treatments

The characterization of potential metabolites plays a determining role in understanding the advancement of T2D ageing. These results were visualized by Rstudio and MetaboAnalyst 5.0. Variable importance in projection (VIP) plot scores were performed to analyze the importance of metabolites under ESI (−/+) modes. Notably, these results showed that metabolites exhibited different distribution trends in the ESI (−/+) modes, and warranting for the importance of employing different ionization modes in LC/MS conditions. In particular, the metabolites of phosphatidylethanolamine lyso 18 and beta-guanidinopropionic acid had the highest values under the ESI- (Fig. 5a) and ESI+ (Fig. 5b), respectively. Interestingly, the phosphatidylethanolamine lyso 18 content in the ULOL group was much higher than that in the other groups. Beta-guanidinopropionic acid, however, played a major role in the model group since it remained at a much higher content than the treatment groups (Fig. 5a and b). To further identify the differential metabolites more intuitively, a volcano plot was generated by Rstudio. 12 and 19 different kinds of metabolites have significantly increased and decreased in the normal group, respectively (Fig. 5c). In contrast, 12 different metabolites were significantly increased, whereas 5 different metabolites were significantly decreased in the Met groups (Fig. 5d). Moreover, the contents of nine (green color circle) and seventeen (red color circle) different metabolites significantly varied in the ULOL groups, respectively. (Fig. 5e). A previous study has shown that supplementing 18-hydroxyeicosapentaenoic acid (18-HEPE) to C57BL/6J mice with a high-fat diet does not reverse hyperglycaemia and insulin deficiency conditions (Pal et al., 2020). Additionally, alpha-D-glucose-1,6-diphosphate, phosphatidylethanolamine lyso 18, all-trans-retinoic acid, 3-acetylindole, and 3′,5′-cyclic AMP were detected in the ULOL group, in which all-trans-retinoic acid and 3′,5′-cyclic AMP have found cell proliferation and differentiation activities in previous studies (Berry et al., 2012; Marasco et al., 2018). Another study found that 3′,5′-cyclic AMP can restore β cells apoptosis

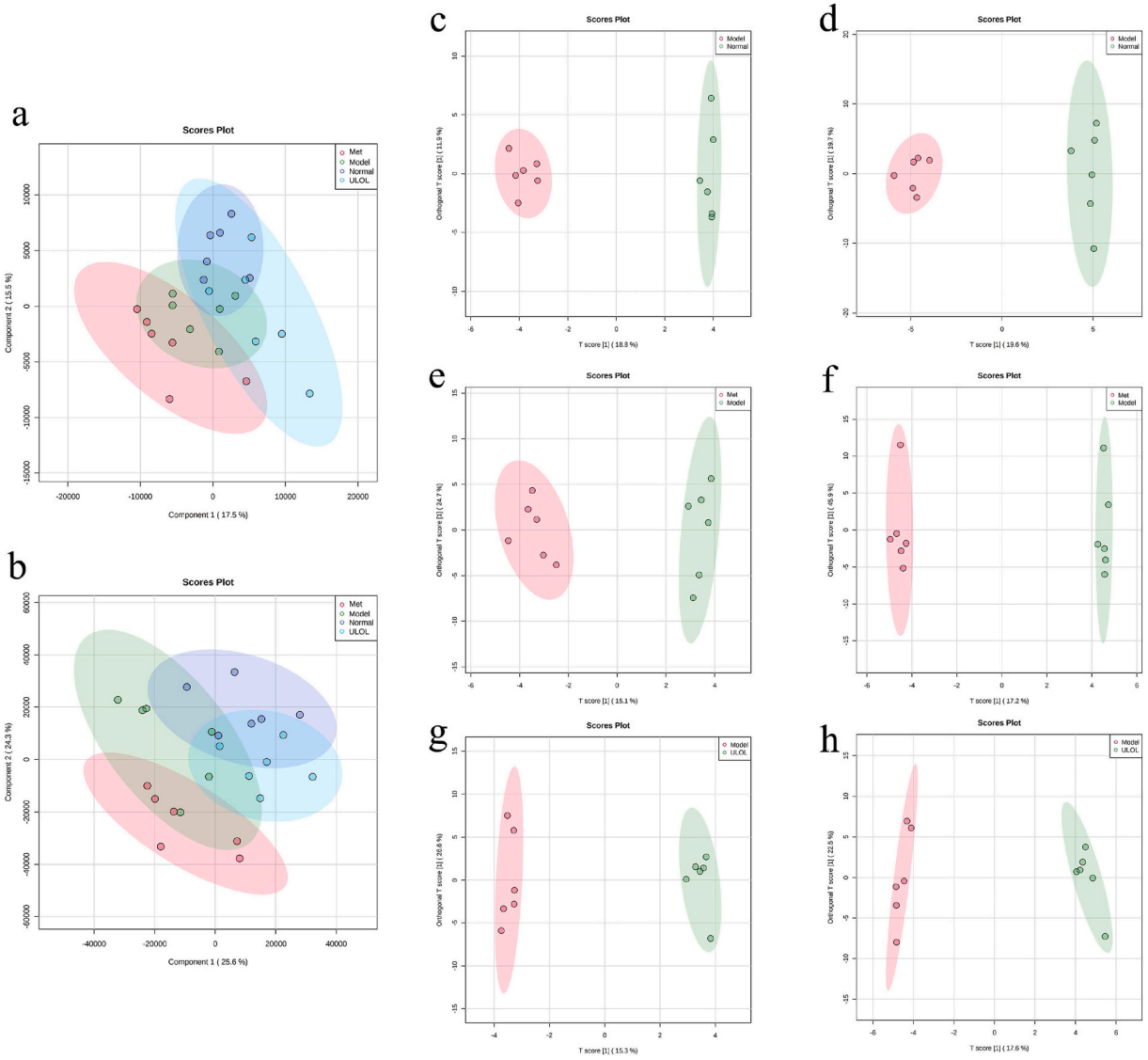


**Fig. 4.** The profiles of brain metabolites analysis of PLS-DA (a & b) and OPLS-DA (c–h). The PLS-DA (a) and OPLS-DA (c & e & g) are under the ESI- modes and PLS-DA (b) and OPLS-DA (d & f & h) are under the ESI + modes. Colored circles indicate 95% confidence intervals.

by regulating $Ca^{2+}$ content and stimulating cell proliferation and differentiation (Bergantin, 2019a,b). Interestingly, all-trans-retinoic acid and 3′,5′-cyclic AMP have similar effectiveness in downregulating inflammatory factors to protect nerves from damage (Bergantin, 2019a,b; Cai et al., 2019). In short, it appears to increase the production of several beneficial endogenous metabolites that aid in delaying the advancement of T2D-ageing conditions in the brain.

### 3.6. Differential metabolic pathways in response to the ULOL

To identify involved metabolic pathways in response to the ULOL intervention in T2D-ageing mice, enrichment analysis using MetaboAnalyst 5.0 mapped to KEGG was performed, and the results revealed that both the pentose phosphate pathway and retinol metabolism were the primary contributors (Fig. 6a and b). The top 50 metabolites in ESI- and ESI+ were selected to distinguish the differential metabolites in each group. Notably, the alpha-D-glucose-1,6-diphosphate showed a distinct positive relationship with the ULOL group (Fig. 6c and d), along with phosphatidylethanolamine lyso 18, all-trans-retinoic acid, 3-acetylindole, spermidine, and 3′,5′-cyclic AMP. Intriguingly, beta-guanidinopropionic acid, and cytidine 5′-diphosphocholine possess a distinct positive relationship in the model group, suggesting that they might be regarded as potential biomarkers for T2D-ageing conditions.

### 3.7. The effects of ULO on gut microbiota variation

The OPLS-DA result revealed the significant segregation between the normal and model groups on opposite sides of the plot, whereas ULO and Met clustered together in the middle along the center line (Fig. 7a). The variational scope of the ULOL group showed similar trends to the Met group as both shared the same coordinate. In addition, these groups showed a different distance, which means that structure of the gut microbiota in T2D-ageing conditions was altered by ULOL and metformin, and different from that in normal group. A linear discriminant analysis (LDA) score was used to examine the variety of different levels in gut microbiota (LDA score>4). The number of microbiota variations in the Met group was distinctly different, especially at seven species levels (Fig. 7b). f_*Streptococcaceae* and g_*Streptococcus* were the primary taxa in the ULOL group. Compared with the normal group, only the f_*Rikenellaceae* occurred in the model group. These results suggest that *Streptococcus* might act as a primary gut microbiota in relieving T2D-ageing conditions following ULOL intervention (Fig. 7c).

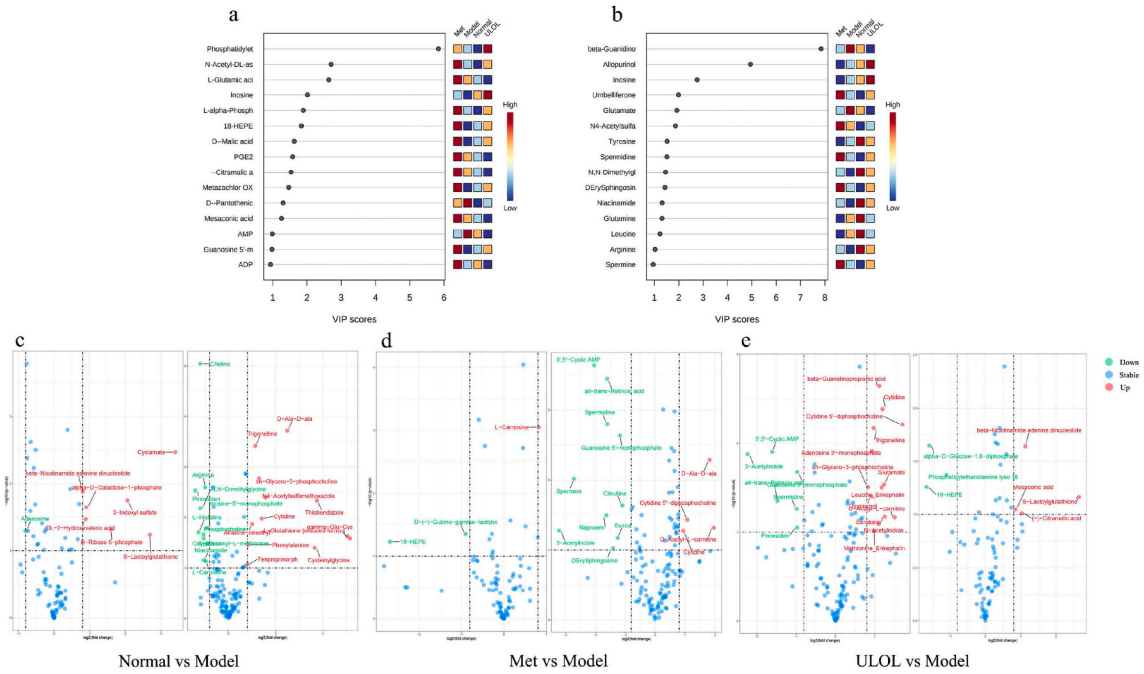


**Fig. 5.** The VIP plot scores from all groups as detected in ESI-(a) and ESI+(b) modes. Green filling means the Model groups downregulation while the contrast groups upregulation and red filling indicate the opposite results. The volcano plot of Normal groups (c), Met group (d) and ULO group (e) each modelled respectively one at a time against Model group as detected in ESI- and ESI+. (For interpretation of the references to color in this figure legend, the reader is referred to the Web version of this article.)

### 3.8. Differential bacterial analysis at the genus level

To distinguish the variation in gut microbiota among the normal, model, Met, and ULOL groups, Welsh's *t*-test calculated the results to reveal the difference after ULO intervention. Notably, nine differential bacteria in the model group were significantly downregulated compared with the normal group (Fig. 8a). Additionally, in the model group, five kinds of bacteria abundance, including *Lactococcus, Enterococcus, Acinetobacter, Corynebacterium,* and *Bilophila,* were upregulated. Six and seven bacteria abundance were enhanced in the Met and ULOL groups, respectively (Fig. 8b and c). Intriguingly, the abundances of *Dubosiella, Oxalobacter,* and *Rikenella* were significantly altered by supplementation with Met and ULOL. Our previous study also observed the abundance changes of *Dubosiella* and *Rikenella* in ULP intervention (Chen et al., 2022), suggesting it may play a potential role in hypoglycaemia and anti-ageing. In addition, the abundances of both Family_XIII_AD3011_group and Family_XIII_UCG-001 seemed to be restored after the supplementation with ULOL, unlike the Model group. Collectively, the abundance of gut microbiota was altered by ULOL intervention, and the beneficial components were maintained to promote gut health.

### 3.9. Correlation analysis between the brain metabolites and gut microbiota

To explore the potential correlation between the brain metabolites and gut microbiota in ULOL group, the results were visualized by TBtools and Cytoscape. As shown in Fig. 9a, *Prevotella* possesses a distinct positive relationship with many brain metabolites except for the 3′,5′-cyclic AMP, spermidine, and all-trans-retinoic acid. By comparison, both 3′,5′-cyclic AMP and all-trans-retinoic acid appeared to be positively correlated with *Bifidobacterium.* Additionally, *Streptococcus*, *Bacteroides*, and Prevotellaceae_NK3B31_group correlated positively with all-trans-retinoic acid. Interestingly, *Desulfovibrio* and *Streptococcus* appeared to be negatively correlated with many metabolites instead of a positive correlation (Fig. 9b). All-trans-retinoic acid correlates positively with *Streptococcus* and *Bifidobacterium,* while the 3′,5′-cyclic AMP observed positive correlation with *Lactobacillus* and *Weissella.* These results suggested that all-trans-retinoic acid and 3′,5′-cyclic AMP might have a positive role for hypoglycaemia and anti-ageing.

## 4. Discussion

Ageing is an important epidemic factor for metabolic-related syndromes and other devasting diseases, such as diabetes, cancer, and cardiovascular disease. Emerging studies have shown that brain dysfunction is a fundamental cause of ageing-related disease prevalence (Liu et al., 2022). Recently, powerful scientific tools have revealed the underlying neurobiological mechanisms of brain-related metabolic regulation. The gut microbiota, which can produce metabolites or proteins to affect the behaviour and metabolism of the host, also mediates these neuropharmacological processes.

Herein, the hypoglycaemia and anti-ageing effects of ULO were evaluated in ageing-related diabetic mice. According to the results revealed that ULO intervention significantly improved FBG levels and glucose tolerance in the ageing-related diabetic mice, and possess more excellent hypoglycaemia activity than metformin intervention. GLP-1/GLP-1R, an important hormones, play a key role in controlling circulating blood glucose in the known brain-gut axis intercommunication (Zanchi et al., 2017). Prior studies have suggested that GLP-1/GLP-1R activation can strengthen the secretion of glucose-dependent insulin and exerts a variety of external pancreas effects to promote antidiabetic effects (Darsalia et al., 2014). In addition, the activation of GLP-1/GLP-1R contributes to control the feeding behavior and balance the diet-associated blood glucose fluctuations in T2D patients (Chen et al., 2022). FoxO1 is a multitarget conservative transcription factor that is involved in apoptosis and autophagy, antioxidant, energy metabolism, and immune regulation (Xing et al., 2018). Evidence has shown that FoxO1 can integrate eating-related neuropeptides in the brain, including proopiomelanocortin and agouti-related protein, to mediate the feeding behavior (Varela and Horvath, 2012). Although there are no direct regulatory relationships among GLP-1, GLP-1R, and FoxO1, they

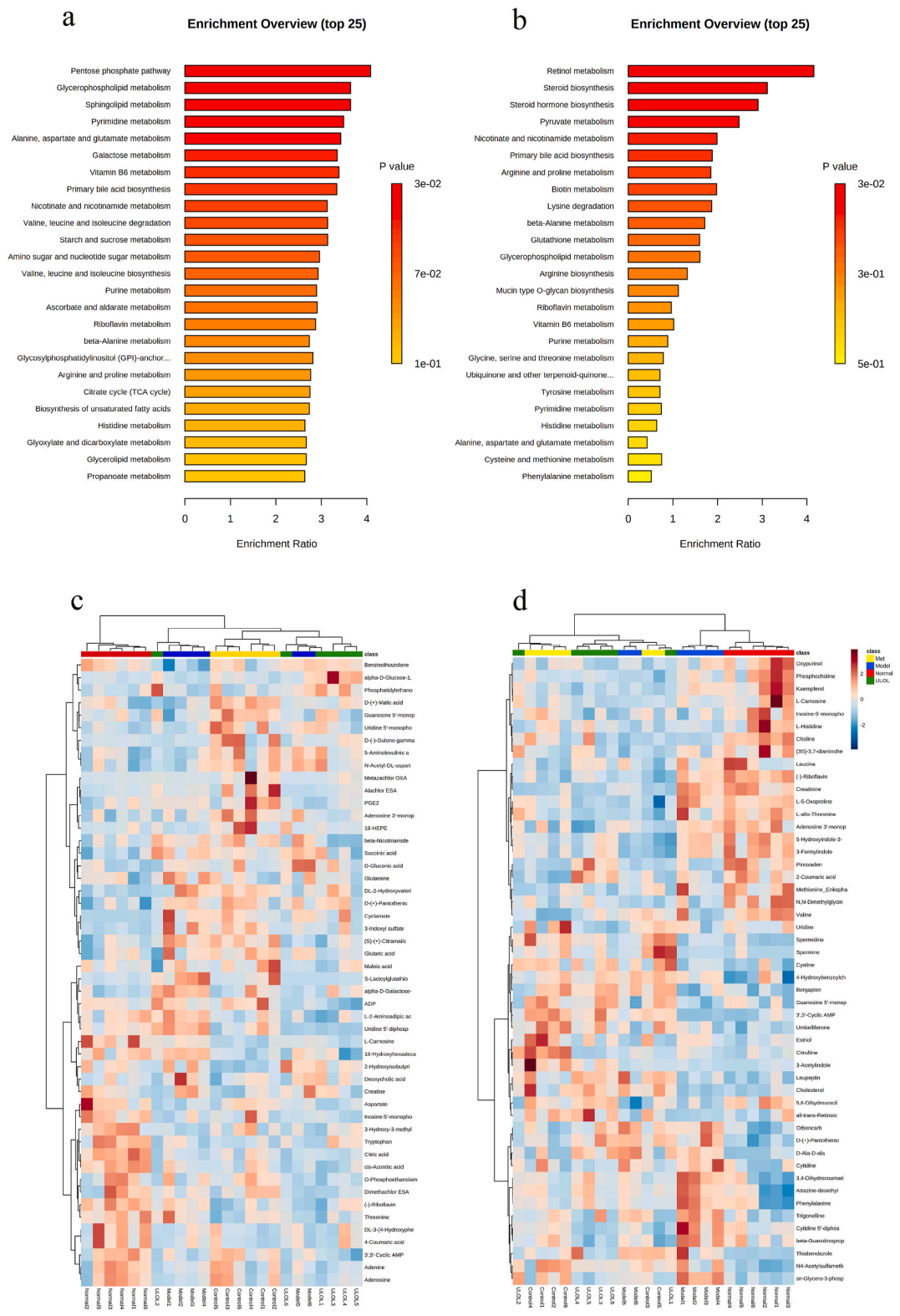


**Fig. 6.** The differential metabolites pathways enrichment (Model vs ULOL) and heatmap analysis of all groups under ESI- (a&c) and ESI+ (b&d) modes.

share common sensitive signals of nutrition and feeding behavior that may contribute to the balance of the diet-associated blood glucose fluctuations. In fact, excessive accumulation of D-galactose could catalyze aldose and hydroperoxide, which aggravate the formation of reactive oxygen species and advanced glycation end products in the brain, resulting in neuronal apoptosis and ATP decrease (Liu et al., 2020). The $p16^{Ink4a}$ and MMP2 are usually overexpressed in senescent cells and tissues, also implying the body in accelerated ageing progression (Grosse et al., 2020; Victoria et al., 2020). Although the mechanism involved in clearance of senescent cells to improve cognitive dysfunction remain elusive, a recent study observed that the downregulation of $p16^{Ink4a}$ and MMP2 can ease ageing-related cognition impairment (Ogrodnik et al., 2021). Additionally, the gut has prominent key roles in maintaining the healthy conditions, especially the bidirectional

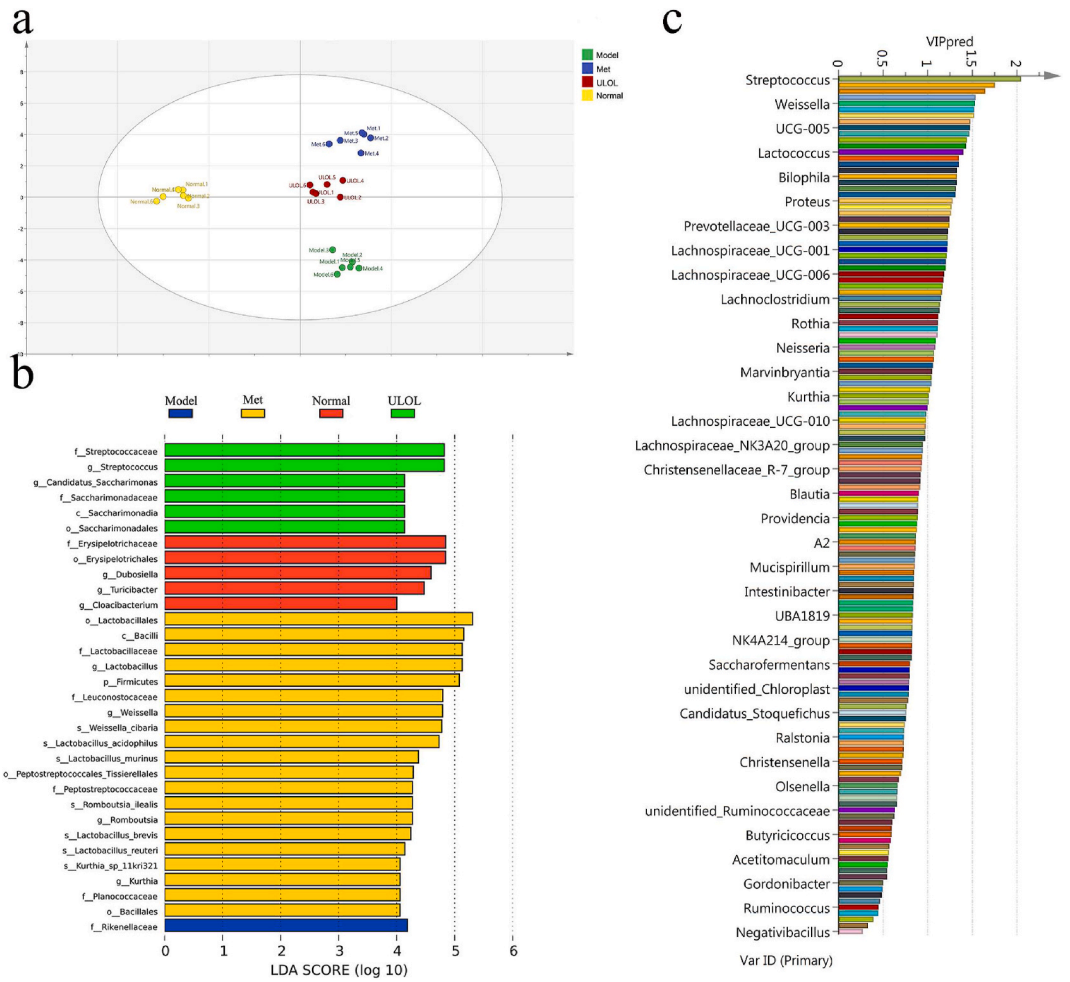


**Fig. 7.** OPLS-DA analysis score plot (a), linear discriminant analysis (LDA) score (b), and VIP score analysis (c).

conduction between the gut and brain regulated immunity, metabolism, and nervous system (Morais et al., 2021). As the core factor in the cellular stress response under diabetes conditions, JNK acts as a signal conductor of insulin resistance that can hamper the insulin synthesis and prevent its action on the substrate, resulting in the conduction limitation of INSR. As such, the GLUT4 is compelled to reduce the absorption and energy conversion of glucose due to the decreased insulin content, leading to an imbalance in blood glucose. In summary, the hypoglycaemia efficiency of ULO is regulated by mediating the expression of INSR, FoxO1, JNK, GLUT4, and GLP-1/GLP-1R, especially the GLP-1/GLP-1R expression involving bidirectional conduction between the gut and brain, which play a key role during the process of hypoglycaemic. Additionally, the activities of $p16^{Ink4a}$ and MMP2 are inhibited by ULO intervention and further hamper the progression of cell senescence.

UPLC-MS-based metabolic analysis is a novel metabolomics tool to investigate the hypoglycaemic and anti-ageing effects of bioactive drugs including oligosaccharides as demonstrated herein. According to our results showed that ULOL intervention was observed to significantly alter brain metabolism. Of note, 26 different metabolites were observed between the model and ULOL groups, including alpha-D-glucose-1,6-diphosphate, phosphatidylethanolamine lyso 18, all-trans-retinoic acid, 3-acetylindole, and 3′,5′-cyclic AMP, etc. Especially, all-trans-retinoic acid and 3′,5′-cyclic AMP have effectiveness in down-regulating inflammatory factors to protect nerves from damage (Bergantin, 2019a,b; Cai et al., 2019). Interestingly, 3′,5′-cyclic AMP can restore β cells apoptosis by regulating $Ca^{2+}$ content and stimulating cell proliferation and differentiation (Bergantin, 2019a,b). A KEGG enrichment analysis revealed that the pentose phosphate pathway and retinol metabolism assumed the major roles following ULOL intervention, involving DNA repair, energy metabolism, and cellular growth. Emerging studies have revealed that the pentose phosphate pathway is highly related to T2D and obesity as a vital part of glucose metabolism, and its flux is enhanced as glycolysis is activated and triggers the production of inflammatory factors to mobilize the inflammatory reaction (Viola et al., 2019). Intriguingly, retinol metabolism also shows a close relationship with diabetes and obesity, especially in the state of diabetes and related diseases, and the dysfunction of the retinol metabolism cascade reveals that it may be a type of disease trigger (Shin et al., 2020). These primary metabolic pathways, including the pentose phosphate pathway and retinol metabolism, showed 4 kinds of metabolites in total, especially with the relative abundance of gluconic acid, which showed fluctuation. Additionally, all-trans-retinoic acid appeared in the differential pathway, which suggested that it plays a crucial role in ageing-related diabetes conditions (Fig. S1).

The gut microbiota plays a crucial role in maintaining metabolic health (Lin et al., 2021b; Shanmugam et al., 2022). The current study showed that ULO has the capacity to regulate gut microbiota structure under ageing-related diabetes conditions. These changes were manifested by upregulating the abundance of *Dubosiella*, *Parasutterella*, *Prevotellaceae*_UCG-001, Family_XIII_AD3011_group, *Oxalobacter*, and *Lachnospiraceae*_UCG-006 and downregulating the abundance of *Rikenella*. *Dubosiella,* of the Firmicutes phylum, is a common bacterium that has been shown to be involved in the production of short-chain fatty acids (SCFAs) and anti-obesity activity (Qiu et al., 2021). *Parasutterella* is regarded as the exporter of succinate that mediates the glycolysis

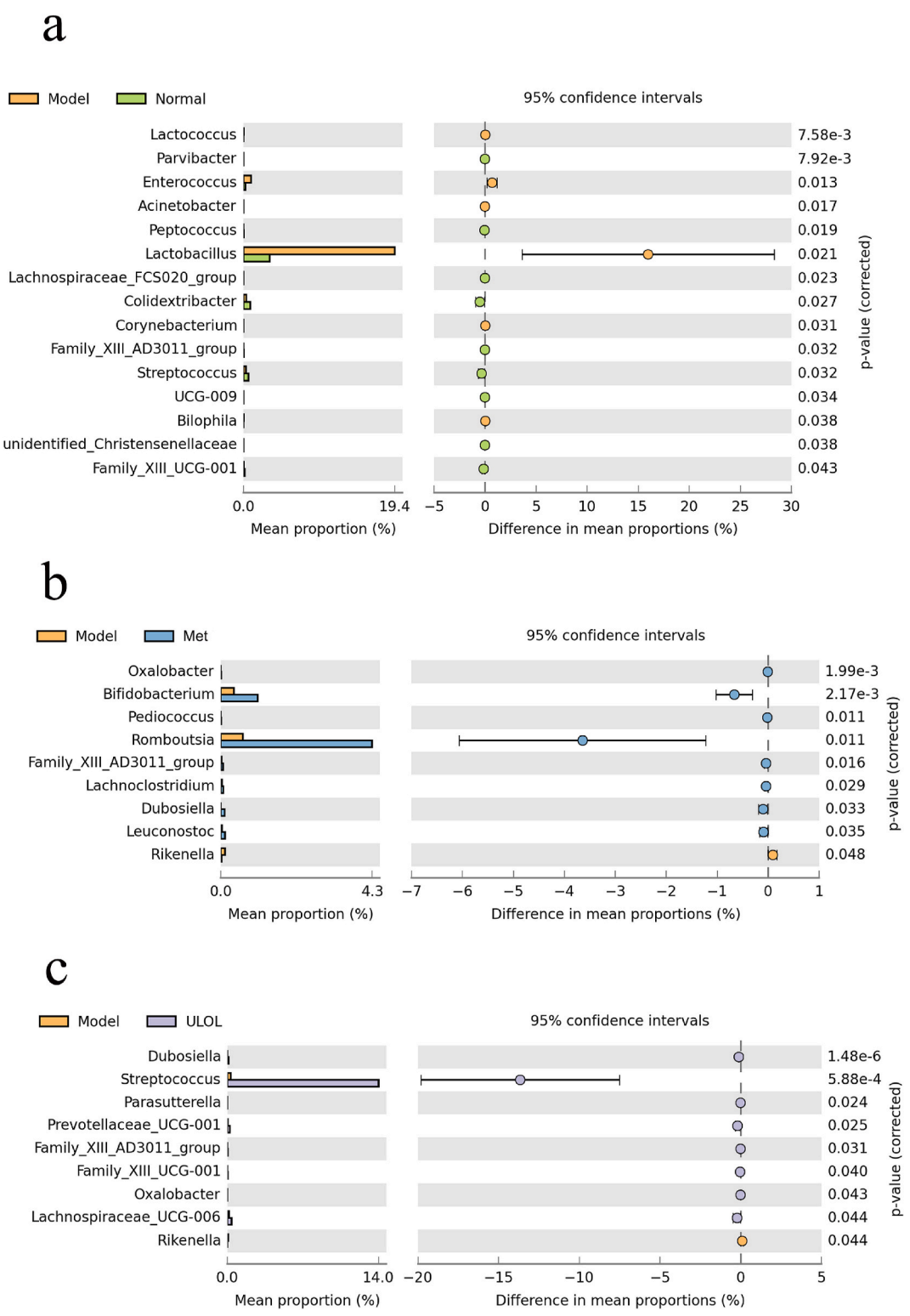


**Fig. 8.** Differential microbiota analysis based on the extended error bar plot (EEBP). Comparison of differential microbiota in Normal (a), Met (b), and ULOL groups (c) compared to the Model group.

process and possesses the underlying capacities of bile acid maintenance and cholesterol metabolism (Ju et al., 2019). *Prevotellaceae*_UCG-001 indicates that there is a close relationship between mediating glucose and lipid metabolism and energy metabolism-related signal regulation. However, the actual effect of these factors needs to be further evaluated (Song et al., 2019). In addition, previous studies have revealed that decreasing the abundance of *Rikenella* has positive effects on the improvement of intestinal barrier function, ageing, diabetes-related diseases, and inflammation (Zhang et al., 2020).

Based on the above analysis, all-trans-retinoic acid, *Streptococcus,* and *Bifidobacterium* have a positive correlation, implying they might play a potentially crucial role in hypoglycaemia and anti-ageing by ULO. Even so, the all-trans-retinoic acid needs to be demonstrated further in ageing-related mice, especially whether they have effective in gut

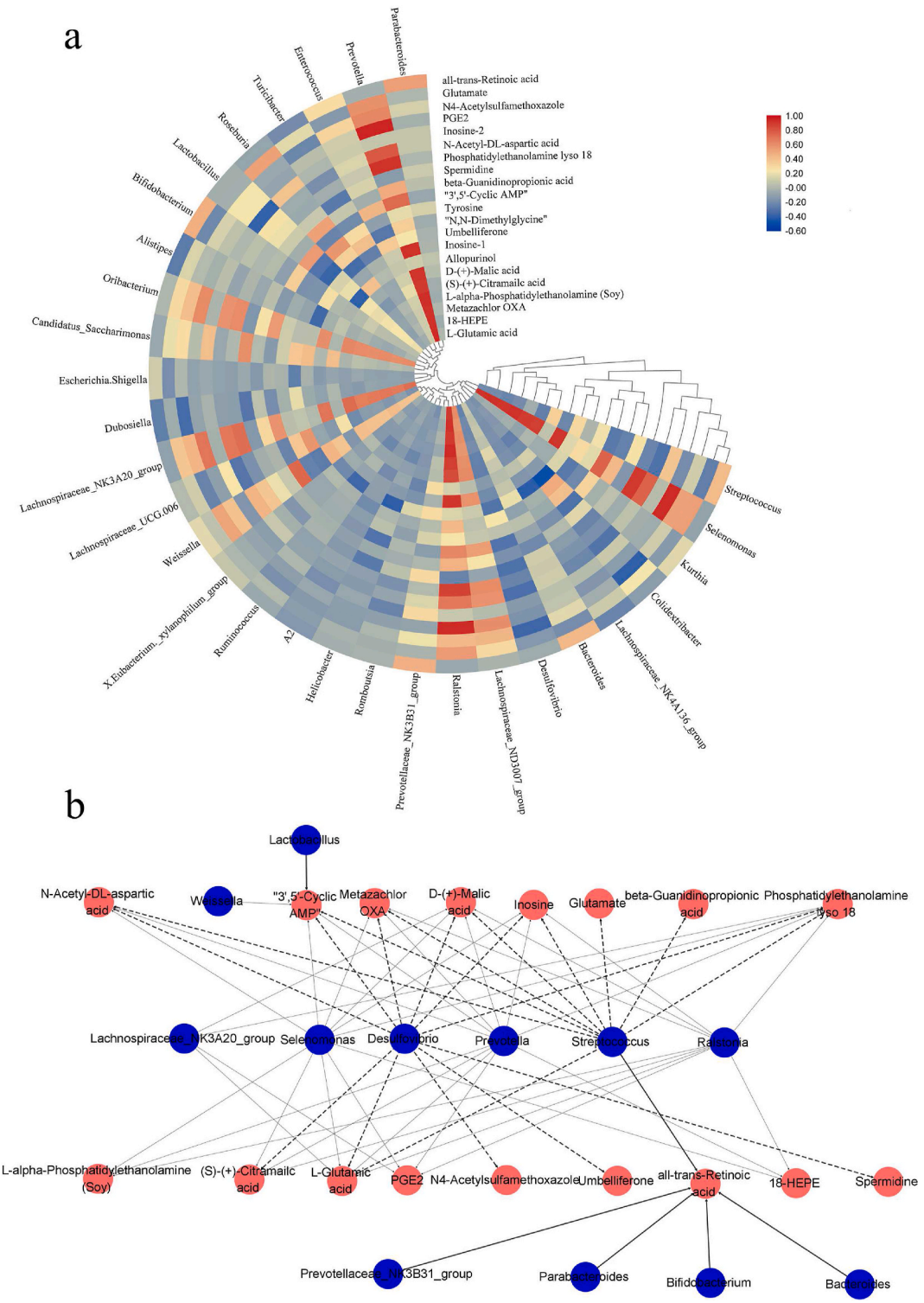


**Fig. 9.** The heatmap analysis is based on the brain metabolites and gut microbiota differential changes in ULOL group (a). The network analysis between the brain metabolites and gut microbiota (b). Solid lines and dotted lines represent positive correlation and negative correlation, respectively.

microbiota regulation.

## 5. Conclusion

A novel oligosaccharide from *U. lactuca* was evaluated in ageing-related diabetic mice herein (Fig. S2). The low dose of ULO (150 mg/kg/d) showed excellent effectiveness of hypoglycaemia than that of metformin intervention, and hampered the overexpression of $p16^{Ink4a}$ and MMP2 to delay the ageing progression in molecular levels. Moreover, ULO also induced the expression of INSR, FoxO1, JNK, GLUT4, and GLP-1/GLP-1R, thereby improving the glucose metabolism status in ageing-related diabetic mice. *Dubosiella*, *Parasutterella*, *Prevotellaceae*_UCG-001, Family_XIII_AD3011_group, *Oxalobacter*, and *Lachnospiraceae*_UCG-006 showed obvious enhances, which is concurrent with downregulate the abundance of *Rikenella*. According to the brain metabolite analysis, all-trans-retinoic acid positively correlates

with *Streptococcus* and *Bifidobacterium*, it might play a potentially crucial role in hypoglycaemia and anti-ageing by ULO. The present work provides an in-depth illustration of the hypoglycaemic and anti-ageing mechanisms of ULO, suggesting that can act as a natural agent to lower the hyperglycaemia and delay senescence.

## Statement

All breeding and experimental protocols followed the ethical regulations of experimental animals, and have been approved by the ethical review of Fujian Agriculture and Forestry University (PZCASFAFU21026).

## CRediT authorship contribution statement

**Yihan Chen:** Methodology, Investigation, Formal analysis, Visualization, Writing – original draft. **Weihao Wu:** Formal analysis, Writing-review, Writing – review & editing. **Xiaoyu Ni:** Formal analysis, Writing-review, Writing – review & editing. **Mohamed A. Farag:** Formal analysis, Writing-review, Writing – review & editing. **Esra Capanoglu:** Formal analysis, Writing-review, Writing – review & editing. **Chao Zhao:** Conceptualization, Resources, Writing – review & editing, Funding acquisition.

## Declaration of competing interest

The authors declare that they have no known competing financial interests or personal relationships that could have appeared to influence the work reported in this paper.

## Acknowledgments

This work was supported by Key Project of the Natural Science Foundation of Fujian Province (2020J02032). The project was also funded by Fujian 'Young Eagle Program' Youth Top Talent Program.

## Appendix A. Supplementary data

Supplementary data to this article can be found online at https://doi.org/10.1016/j.crfs.2022.07.003.

## References

Agunloye, O.M., Oboh, G., 2022. Blood glucose lowering and effect of oyster (*Pleurotus ostreatus*)-and shiitake (*Lentinus subnudus*)-supplemented diet on key enzymes linked diabetes and hypertension in streptozotocin-induced diabetic in rats. Food Front 3 (1), 161–171.
Beraza, N., Trautwein, C., 2008. The gut-brain-liver axis: a new option to treat obesity and diabetes? Hepatology 48 (3), 1011–1013.
Bergantin, L.B., 2019a. Diabetes and cancer: debating the link through $Ca^{2+}$/cAMP signaling. Curr. Diabetes Rev. 16 (3), 238–241.
Bergantin, L.B., 2019b. Hypertension, diabetes and neurodegenerative diseases: is there a clinical link through the $Ca^{2+}$/cAMP signalling interaction? Curr. Hypertens. Rev. 15 (1), 32–39.
Berry, D.C., O'Byrne, S.M., Vreeland, A.C., Blaner, W.S., Noy, N., 2012. Cross talk between signaling and vitamin a transport by the retinol-binding protein receptor STRA6. Mol. Cell Biol. 32 (15), 3164–3175.
Bosco, D., Plastino, M., Cristiano, D., Colica, C., Ermio, C., De Bartolo, M., Mungari, P., Fonte, G., Consoli, D., Consoli, A., Fava, A., 2012. Dementia is associated with insulin resistance in patients with Parkinson's disease. J. Neurol. Sci. 315 (1–2), 39–43.
Cai, W., Wang, J.L., Hu, M.Y., Chen, X., Lu, Z.Q., Bellanti, J.A., Zheng, S.G., 2019. All trans-retinoic acid protects against acute ischemic stroke by modulating neutrophil functions through STAT1 signaling. J. Neuroinflammation 16 (1), 175.
Chen, Y., Ouyang, Y., Chen, X., Chen, R., Ruan, Q., Farag, M.A., Chen, X., Zhao, C., 2022. Hypoglycaemic and anti-ageing activities of green alga *Ulva lactuca* polysaccharide via gut microbiota in ageing-associated diabetic mice. Int. J. Biol. Macromol. 212, 97–110.
Darsalia, V., Nathanson, D., Nyström, T., Klein, T., Sjöholm, Å., Patrone, C., 2014. GLP-1R activation for the treatment of stroke: updating and future perspectives. Rev. Endocr. Metab. Disord. 15 (3), 233–242.
Ghislain, J., Poitout, V., 2021. Targeting lipid GPCRs to treat type 2 diabetes mellitus-progress and challenges. Nat. Rev. Endocrinol. 17 (3), 162–175.
Grosse, L., Wagner, N., Emelyanov, A., Molina, C., Lacas-Gervais, S., Wagner, K.D., Bulavin, D.V., 2020. Defined $p16^{High}$ senescent cell types are indispensable for mouse healthspan. Cell Metabol. 32 (1), 87–99 e6.
Guasch-Ferré, M., Hruby, A., Toledo, E., Clish, C.B., Martínez-González, M.A., Salas-Salvadó, J., Hu, F.B., 2016. Metabolomics in prediabetes and diabetes: a systematic review and meta-analysis. Diabetes Care 39 (5), 833–846.
Gupta, A., Osadchiy, V., Mayer, E.A., 2020. Brain–gut–microbiome interactions in obesity and food addiction. Nat. Rev. Gastroenterol. Hepatol. 17 (11), 655–672.
Huang, Y., Chen, Y., Lu, S., Zhao, C., 2021. Recent advance of *in vitro* models in natural phytochemicals absorption and metabolism. eFood 2 (6), 307–318.
Hwang, A.B., Ryu, E.A., Artan, M., Chang, H.W., Kabir, M.H., Nam, H.J., Lee, D., Yang, J. S., Kim, S., Mair, W.B., Lee, C., Lee, S.S., Lee, S.J., 2014. Feedback regulation via AMPK and HIF-1 mediates ROS-dependent longevity in *Caenorhabditis elegans*. Proc. Natl. Acad. Sci. U.S.A. 111 (42), E4458–E4467.
Ju, T., Kong, J.Y., Stothard, P., Willing, B.P., 2019. Defining the role of *Parasutterella*, a previously uncharacterized member of the core gut microbiota. ISME J. 13 (6), 1520–1534.
Kaplan, L., Chow, B.W., Gu, C., 2020. Neuronal regulation of the blood–brain barrier and neurovascular coupling. Nat. Rev. Neurosci. 21 (8), 416–432.
Lin, G.P., Wan, X.Z., Liu, D., Wen, Y.X., Yang, C.F., Zhao, C., 2021a. COL1A1 as a potential new biomarker and therapeutic target for type 2 diabetes. Pharmacol. Res. 165, 105436.
Lin, H., Zhang, J., Li, S., Zheng, B., Hu, J., 2021b. Polysaccharides isolated from *Laminaria japonica* attenuates gestational diabetes mellitus by regulating the gut microbiota in mice. Food Front 2, 208–217.
Liu, H., Zhang, X.G., Xiao, J., Song, M.Y., Cao, Y., Xiao, H., Liu, X.J., 2020. Astaxanthin attenuates d-galactose-induced brain aging in rats by ameliorating oxidative stress, mitochondrial dysfunction, and regulating metabolic markers. Food Funct. 11 (5), 4103–4113.
Liu, T., Xu, Y., Yi, C.X., Tong, Q., Cai, D., 2022. The hypothalamus for whole-body physiology: from metabolism to aging. Protein Cell 13 (6), 394–421.
Liu, X.Y., Liu, D., Lin, G.P., Wu, Y.J., Gao, L.Y., Ai, C., Huang, Y.F., Wang, M.F., El-Seedi, H.R., Chen, X.H., Zhao, C., 2019. Anti-ageing and antioxidant effects of sulfate oligosaccharides from green algae *Ulva lactuca* and *Enteromorpha prolifera* in SAMP8 mice. Int. J. Biol. Macromol. 139, 342–351.
Marasco, M.R., Conteh, A.M., Reissaus, C.A., Cupit, J.E. 5th, Appleman, E.M., Mirmira, R. G., Linnemann, A.K., 2018. Interleukin-6 reduces β-cell oxidative stress by linking autophagy with the antioxidant response. Diabetes 67 (8), 1576–1588.
Morais, L.H., Schreiber, H.L. 4th, Mazmanian, S.K., 2021. The gut microbiota-brain axis in behaviour and brain disorders. Nat. Rev. Microbiol. 19 (4), 241–255.
Nauck, M.A., Vilsbøll, T., Gallwitz, B., Garber, A., Madsbad, S., 2009. Incretin-based therapies: viewpoints on the way to consensus. Diabetes Care 2 (Suppl. 2), S223–S231, 32Suppl.
Ogrodnik, M., Evans, S.A., Fielder, E., Victorelli, S., Kruger, P., Salmonowicz, H., Weigand, B.M., Patel, A.D., Pirtskhalava, T., Inman, C.L., Johnson, K.O., Dickinson, S.L., Rocha, A., Schafer, M.J., Zhu, Y., Allison, D.B., von Zglinicki, T., LeBrasseur, N.K., Tchkonia, T., Neretti, N., Passos, J.F., Kirkland, J.L., Jurk, D., 2021. Whole-body senescent cell clearance alleviates age-related brain inflammation and cognitive impairment in mice. Aging Cell 20 (2), e13296.
Osadchiy, V., Martin, C.R., Mayer, E.A., 2019. The gut–brain axis and the microbiome: mechanisms and clinical implications. Clin. Gastroenterol. Hepatol. 17 (2), 322–332.
Pal, A., Al-Shaer, A.E., Guesdon, W., Torres, M.J., Armstrong, M., Quinn, K., Davis, T., Reisdorph, N., Neufer, P.D., Spangenburg, E.E., Carroll, I., Bazinet, R.P., Halade, G. V., Clària, J., Shaikh, S.R., 2020. Resolvin E1 derived from eicosapentaenoic acid prevents hyperinsulinemia and hyperglycemia in a host genetic manner. Faseb. J. 34 (8), 10640–10656.
Qiu, X., Macchietto, M.G., Liu, X., Lu, Y., Ma, Y., Guo, H., Saqui-Salces, M., Bernlohr, D. A., Chen, C., Shen, S., Chen, X., 2021. Identification of gut microbiota and microbial metabolites regulated by an antimicrobial peptide lipocalin 2 in high fat diet-induced obesity. Int. J. Obes. 45 (1), 143–154.
Scherz-Shouval, R., Elazar, Z., 2011. Regulation of autophagy by ROS: physiology and pathology. Trends Biochem. Sci. 36 (1), 30–38.
Serag, A., Shakkour, Z., Halboup, A.M., Kobeissy, F., Farag, M.A., 2021. Sweat metabolome and proteome: recent trends in analytical advances and potential biological functions. J. proteomics. 246, 104310.
Shanmugam, H., Ganguly, S., Priya, B., 2022. Plant food bioactives and its effects on gut microbiota profile modulation for better brain health and functioning in autism spectrum disorder individuals: a review. Food Front 3, 124–141.
Shin, S.J., Chen, C.H., Kuo, W.C., Chan, H.C., Chan, H.C., Lin, K.D., Ke, L.Y., 2020. Disruption of retinoid homeostasis induces RBP4 overproduction in diabetes: O-GlcNAcylation involved. Metabolism 113, 154403.
Sinclair, Saeedi, P., Kaundal, A., Karuranga, S., Malanda, B., Williams, R., 2020. Diabetes and global ageing among 65-99-year-old adults: findings from the international diabetes federation diabetes atlas. Diabetes Res. Clin. Pract. 162, 108078 ninth ed.
Song, X., Zhong, L., Lyu, N., Liu, F., Li, B., Hao, Y., Xue, Y., Li, J., Feng, Y., Ma, Y., Hu, Y., Zhu, B., 2019. Inulin can alleviate metabolism disorders in ob/ob mice by partially restoring leptin-related pathways mediated by gut microbiota. Dev. Reprod. Biol. 17 (1), 64–75.
Teferra, T.F., 2021. Possible actions of inulin as prebiotic polysaccharide: a review. Food Front 2, 407–416.
Tundis, R., 2021. Contribution of bioactive compounds from Mediterranean plant foods in promoting health effects: a profile of Rosa Tundis. Food Front 2, 91–92.
Varela, L., Horvath, T.L., 2012. Leptin and insulin pathways in POMC and AgRP neurons that modulate energy balance and glucose homeostasis. EMBO Rep. 13 (12), 1079–1086.

Victoria, E.C.G., Toscano, E.C.B., Oliveira, F.M.S., de Carvalho, B.A., Caliari, M.V., Teixeira, A.L., de Miranda, A.S., Rachid, M.A., 2020. Up-regulation of brain cytokines and metalloproteinases 1 and 2 contributes to neurological deficit and brain damage in transient ischemic stroke. Microvasc. Res. 129, 103973.

Viola, A., Munari, F., Sanchez-Rodriguez, R., Scolaro, T., Castegna, A., 2019. The metabolic signature of macrophage responses. Front. Immunol. 10, 1462.

Wan, X.Z., Ai, C., Chen, Y.H., Gao, X.X., Zhong, R.T., Liu, B., Chen, X.H., Zhao, C., 2020. Physicochemical characterization of a polysaccharide from green microalga *chlorella pyrenoidosa* and its hypolipidemic activity via gut microbiota regulation in rats. J. Agric. Food Chem. 68 (5), 1186–1197.

Wu, D.S., Chen, Y.H., Wan, X.Z., Liu, D., Wen, Y.X., Chen, X.H., Zhao, C., 2020. Structural characterization and hypoglycemic effect of green alga *Ulva lactuca* oligosaccharide by regulating microRNAs in *Caenorhabditis elegans*. Algal Res. 51, 102083.

Xing, Y.Q., Li, A., Yang, Y., Zhang, L.N., Guo, H.C., 2018. The regulation of FOXO1 and its role in disease progression. Life Sci. 193, 124–131.

Zanchi, D., Depoorter, A., Egloff, L., Haller, S., Mählmann, L., Lang, U.E., Drewe, J., Beglinger, C., Schmidt, A., Borgwardt, S., 2017. The impact of gut hormones on the neural circuit of appetite and satiety: a systematic review. Neurosci. Biobehav. Rev. 80, 457–475.

Zhang, Y.W., Chen, L.Y., Hu, M.J., Kim, J.J., Lin, R.B., Xu, J.L., Fan, L.N., Qi, Y.D., Wang, L., Liu, W.L., Deng, Y.Y., Si, J.M., Chen, S.J., 2020. Dietary type 2 resistant starch improves systemic inflammation and intestinal permeability by modulating microbiota and metabolites in aged mice on high-fat diet. Aging 12 (10), 9173–9187.

Zhao, C., Lin, G.P., Wu, D.S., Liu, D., You, L.J., Högger, P., Simal−Gandara, J., Wang, M. F., da Costa, J.G.M., Marunaka, Y., Daglia, M., Khan, H., Filosa, R., Wang, S.Y., Xiao, J.B., 2020a. The algal polysaccharide ulvan suppresses growth of hepatoma cells. Food Front 1 (1), 83–101.

Zhao, C., Wan, X.Z., Zhou, S., Cao, H., 2020b. Natural polyphenols: a potential therapeutic approach to hypoglycemia. eFood 1 (2), 107–118.

Zhao, C., Lai, S.S., Wu, D.S., Liu, D., Zou, X.B., Ismail, A., El-Seedi, H., Arroo, R.J., Xiao, J.B., 2020c. miRNAs as regulators of antidiabetic effects of fucoidans. eFood 1 (1), 2–11.